

# Deuterated Clathrate Hydrates as a Novel Moderator Material for Very Cold Neutrons. Project Aperçu and First Results.

Valentin Czamler<sup>1,2,\*</sup>, Thomas C. Hansen<sup>2</sup>, Michael Marek Koza<sup>2</sup>, Richard Wagner<sup>2</sup>, and Oliver Zimmer<sup>2</sup>

<sup>1</sup>École Doctorale de Physique, Université Grenoble Alpes, 38402 Saint Martin d'Hères, France

<sup>2</sup>Institut Laue-Langevin (ILL), 71 Avenue des Martyrs, 38042 Grenoble Cedex 9, France

**Abstract.** Clathrate hydrates are water-based solids with large crystallographic unit cells that show promise as potential moderators for use in new, more intense sources of very cold neutrons (VCN), which would enhance neutron scattering techniques and increase sensitivity of particle physics experiments. These so-called inclusion compounds seem particularly suitable for this application due to the low-energy modes of guest molecules engaged in nano-voids formed by a crystalline network of hydrogen bonded water molecules. In this article we present first results of an ongoing, extensive experimental campaign with the aim of characterizing the scattering properties of deuterated clathrate hydrates relevant for moderator applications. Experiments include neutron diffraction (carried out at Institut Laue-Langevin (ILL) using the instrument D20), as well as measurements of the temperature-dependent dynamical structure factor  $S(q, \omega)$  in absolute units (carried out on ILL's Panther and IN5). These measurements will serve as a benchmark for development of new scattering kernels.

## 1 Introduction

Very cold neutrons (VCN) cover a wide spectral range within the long-wavelength tail of typical sources for cold neutrons<sup>1</sup>, with energies below, say, 1 meV (9 Å) down to few hundreds of neV (> several 100 Å), the domain of ultracold neutrons (UCN). Notably wavelengths of up to several tens of Å are in the focus of current interest of several research communities. In condensed matter physics, they serve as a sensitive probe and could improve multiple neutron scattering techniques in terms of spacial resolution as e.g. for small angle neutron scattering (SANS), or energy resolution as e.g. in time of flight (TOF) or neutron spin echo (NSE) spectrometers [1]. In particle physics, higher VCN intensities would increase the sensitivity of experiments that employ beams of slow neutrons. Examples are the search for neutron anti-neutron oscillations [2], where the figure of merit (FOM)  $\propto \lambda^2$ , in-beam searches for a static neutron electric dipole moment (EDM), and further searches for new fundamental forces where FOM  $\propto \lambda$  [3] [4]. Furthermore, an enhancement of the flux of neutrons with wavelengths around 9 Å would be a valuable asset for in-beam UCN-sources based on super-fluid helium [5], including variants with in-situ UCN production and detection approaches, as proposed in [6]. Despite the scientific potentials of VCN beams, at present the only existing VCN beamline is the instrument PF2 located at the Institut Laue-Langevin (ILL) in Grenoble, France. At this instrument, the vertical extrac-

tion by a strongly curved neutron guide from one of ILL's cold sources transmits only the long-wavelength tail of the liquid-deuterium moderator spectrum. In order to realize higher fluxes of VCN, additional moderation to lower temperatures seems inevitable, which strongly motivates the search for appropriate, new moderator materials.

### 1.1 Required properties of novel cold and very cold moderator materials

The moderating properties of a material are practically determined by its excitation spectrum and its coupling strength to the neutron field via the cross section. Thus, promising materials for moderation to VCN need to possess low-energy modes that enable the incremental deposition of small quantities of the neutron's energy. This can hardly be provided by collective excitations such as phonons since their cross section, for a neutron of energies  $E < k_B T_D$ , in a cold medium with the Debye temperature  $T_D$  is proportional to  $(\frac{E}{k_B T_D})^3$  (for single phonon emission<sup>2</sup>) [7]. Localized, dispersion-free excitations, such as displacement of confined molecules, often referred to as Einstein modes, molecular rotations, librations or paramagnetic excitations, on the other hand, do not suffer from this limitation and allow for an efficient neutron slowdown even at lowest neutron temperatures. Besides suitable localized excitations, the material needs to exhibit low absorption and large scattering cross sections in the corresponding energy and temperature region. In addition, a moderator material must also fulfill more technical requirements. If its thermal conductivity is low, the material

\*e-mail: vczamler@ill.fr

<sup>1</sup>The standard cold moderator materials for both spallation and fission sources are liquid or solid deuterium (D<sub>2</sub>), liquid hydrogen (H<sub>2</sub>) and liquid or solid hydrocarbons (e.g. methane (CH<sub>4</sub>)).

<sup>2</sup>The cross sections for processes of higher order drop even faster.

must be arranged in a manner that enables efficient cooling. On top of that it must withstand radiational damage to a degree that prevents the formation of radiolytic hydrogen as well as the accumulation of free radicals. This could result in a self-sustaining reaction of their recombination leading to a fast heating of the moderator, often referred to as "burp" [8] [9] [10]. In this article we present parts of an extensive inelastic neutron scattering study on different clathrate hydrate samples carried out on various neutron scattering instruments at the ILL.

## 1.2 A promising material class: Fully deuterated clathrate hydrates

Promising moderator materials investigated so far are different hydrocarbons, such as triphenylmethane [11], mesitylene and toluene [12], as well as clathrate hydrates [13] hosting methane or tetrahydrofuran (THF) [14]. Mesitylene is already in routine usage in form of a pelletized cold moderator at the IBR-2M reactor in Dubna [15]. This article focuses on the latter material class, where the encaged guest molecules provides a range of localized, low-energy excitations that can be exploited for neutron slowdown. Given their very large crystallographic unit cells (as in the case of the clathrate structure II (CS-II)  $17.1 \text{ \AA} - 17.33 \text{ \AA}$ , see table 1), which allows for coherent scattering up to neutron wavelengths of  $\lambda \sim 20 \text{ \AA}$ , these materials promise extraordinarily large albedos for the entire cold neutron range. This allows neutrons that did not scatter down to the desired energy range to be "trapped" within the moderator material by diffuse transport, thus largely increasing the chance for further, energy decreasing interactions.

In this work, we present a study of clathrate hydrates hosting tetrahydrofuran as a guest molecule (sum formula:  $17\text{H}_2\text{O}:\text{C}_4\text{H}_8\text{O}$ ), from here on referred to as THF-hydrates. A great advantage of this type of hydrate is its very reliable and reproducible manufacturing from a stoichiometric mixture under ambient pressure (see section 2.1). This would even allow for an in-situ annealing, thus re-establishing the clathrate structure within the moderator volume, in order to prevent a "burp" of the moderator due to radiolysis. To some extent, the low-energy excitations of THF-hydrates have already been studied [14] [16]. We have extended those studies to include deuterated materials, and to cover  $S(q, \omega)$  in a large energy-momentum phase space in absolute units, which is essential for a quantitative analysis of the moderation properties in realistic scenarios.

While fully deuterated THF-hydrates ( $17\text{D}_2\text{O}:\text{C}_4\text{D}_8\text{O}$ ) by themselves show very promising properties as a moderator material for VCN, they are also a good starting material for the formation of binary clathrate hydrates with both THF and molecular oxygen as guest molecules ( $17\text{D}_2\text{O}:\text{C}_4\text{D}_8\text{O}:\sim 2\text{O}_2$ ).<sup>3</sup> Therein,  $\text{O}_2$  occupies the small cages, which are twice as abundant as the bigger cages occupied by the TDF. The magnetic triplet ground state of

<sup>3</sup>The oxygen abundance is, unlike the  $\text{C}_4\text{D}_8\text{O}$  (TDF), non-stoichiometric and strongly depends on the sample preparation. This is represented by "~".

molecular oxygen with its zero-field splitting of  $0.4 \text{ meV}$  allows for moderation via a cooling cascade mechanism in fully deuterated  $\text{O}_2$ -clathrate hydrates, as described in [17]. It is this low excitation energy (as opposed to modes of several  $\text{meV}$  of the lattice and the THF) that will significantly enhance the moderation efficiency towards VCN, with the inelastic magnetic scattering providing a final cooling decrement.

## 1.3 Development of new scattering kernels in the HighNESS project

The study of novel VCN moderator materials is part of a collaborative effort within the European project HighNESS [18], committed to expanding the scientific potential of the European Spallation Source (ESS), by exploring new possible sources of slow neutrons. One of the goals is to establish a database of the dynamic structure factor  $S(q, \omega)$  for various promising clathrate hydrates and to develop novel scattering kernels that allow computation of neutron spectra in realistic moderator and reflector geometries in Monte Carlo (MC) simulations (see also Ref. [19]). To this end, the experimental campaign is accompanied by the development of simulation software to describe neutron interactions in materials that we investigate. The approach is to benchmark the excitation spectrum from ab initio molecular dynamics (MD) calculations, with the experimental data presented in this article. In combination with processing codes, such as NJOY [20] and NCrystal [21], this allows the creation of scattering kernels that are callable from McStas [22], OpenMC [23], MCNP [24] or PHITS [25]. This provides the tools to simulate novel moderator and reflector materials in realistic geometries, and compare simulations with results of experiments to be performed on a later stage using a large bulk of material as a demonstrator of a VCN moderator.

## 2 Experimental Programm

A starting point of the experiments described here is establishing a reliable and scalable technique, that allows production of relatively large quantities of hydrates with minimal amounts of residual ice. This technique is described for THF-hydrates in section 2.1. The obtained structures were studied by neutron diffraction at the high-intensity two-axis diffractometer D20. An exemplary powder pattern and details of the associated Rietveld-refinement are given in section 2.2. The structure analysis is followed by a study of the low-energy dynamics of different THF-hydrate samples, as described in 2.3. The data presented in this article were collected during cycles  $\text{N}^\circ 189$ ,  $\text{N}^\circ 190$  and  $\text{N}^\circ 191$  at the ILL.

### 2.1 Manufacturing procedures

A great advantage of THF-hydrates, compared to most other clathrate hydrate compounds, is that they form at ambient conditions from a stoichiometric mixture of its two liquid components, water ( $\text{H}_2\text{O}$ ) and THF ( $\text{C}_4\text{H}_8\text{O}$ ),

in a ratio of 17 to 1. After carefully weighing and mixing the two liquids with a teflon-coated magnetic stirrer, a cool-down of the solution results in solidification in the CS-II structure (see table 1). The CS-II structure is the most common among clathrate hydrates and its ideal unit cell contains 136 ( $\text{H}_2\text{O}$ ) molecules forming 16 small and 8 large cages. This structure has been extensively studied before (see e.g. [26]). The study presented here focuses on the yields of the CS-II structure and quantifying the residual ice, for two different methods to cool down the sample. A great advantage of the manufacturing technique is, that

Crystal system	Cubic
Space group	Fd3m (N°227)
Lattice description	Face centered
F Lattice parameters	$a = 17.1 \text{ \AA} - 17.33 \text{ \AA}$ $\alpha = \beta = \gamma = 90^\circ$
Number of cages	8 large ( $5^{12} 6^4$ ), 16 small ( $5^{12}$ )
Ideal unit cell formula	$8(5^{12} 6^4) \cdot 16(5^{12}) \cdot 136\text{H}_2\text{O}$

Table 1: Characteristics of the CS-II hydrate crystal cell structure. In the case of THF-hydrates the unit cell formula reduces to 8 THF:136  $\text{H}_2\text{O}$ , with the small cages remaining empty. Table adapted from [27, p. 60].

it allows to perform a contrast variation between the host and the guest contribution in spectroscopy experiments. By simply substituting one of the liquid components with its deuterated counterpart (water ( $\text{H}_2\text{O}$ ) with heavy water ( $\text{D}_2\text{O}$ ) and THF ( $\text{C}_4\text{H}_8\text{O}$ ) with TDF ( $\text{C}_4\text{D}_8\text{O}$ )) one obtains four different samples which are summarized in table 2.

	Abbrev.	Host	Guest
Fully protonated	THF · $\text{H}_2\text{O}$	136 $\text{H}_2\text{O}$	8 $\text{C}_4\text{H}_8\text{O}$
Deuterated guest	TDF · $\text{H}_2\text{O}$	136 $\text{H}_2\text{O}$	8 $\text{C}_4\text{D}_8\text{O}$
Deuterated cage	THF · $\text{D}_2\text{O}$	136 $\text{D}_2\text{O}$	8 $\text{C}_4\text{H}_8\text{O}$
Fully deuterated	TDF · $\text{D}_2\text{O}$	136 $\text{D}_2\text{O}$	8 $\text{C}_4\text{D}_8\text{O}$

Table 2: Differently deuterated and protonated samples prepared for spectroscopy experiments. The deuteration of either the guest molecule or the host lattice allows to highlight the different parts of the sample in the scattering signal. Note that the fully or partial deuteration is able to slightly change the dynamics of the sample, while the structure remains the one described in table 1.

## 2.2 Neutron diffraction on fully deuterated THF-hydrates

The diffractometer was operated using the (115) reflection of a Germanium(113) monochromator at a wavelength of  $\lambda = 1.546 \text{ \AA}$ , at a take off angle of  $90^\circ$  resulting in a resolution of  $\Delta d/d = 3 \cdot 10^{-3}$ . The cylindrical sample container made from vanadium (with a diameter of 6 mm and a wall thickness of 0.1 mm) was filled with the liquid stoichiometric mixture and quenched in liquid nitrogen before being loaded into the cryogenic sample environment. After equilibration to a set temperature value, it took about

30 minutes to obtain a diffraction pattern within a scattering angle range of  $4^\circ$  to  $150^\circ$  with satisfactory statistics. This allowed measurements within a temperature range of 2 K - 230 K. Afterwards, the sample was heated up above the melting point ( $\sim 277.5 \text{ K}$ ) and slowly (about 7 K per minute) cooled down again below 200 K. We observed that the CS-II structure is formed through both rapid quenching and slower cooling of the liquid sample. Effects of texture of the polycrystalline samples were observed as a dependence of diffraction patterns on sample orientation (which for an ideal powder would be absent). They are inherent for an uncontrolled in-situ crystallization, which can lead to a small number of crystallites and ultimately to a deviation from continuous powder lines (towards single points on the Debye-Scherrer cones). Mitigation of this effect was attempted by rotating the sample in increments of  $20^\circ$  and adding up the resulting 9 diffraction patterns, for better approximation of a powder average. Figure 1 shows an exemplary diffraction pattern obtained with this procedure at a temperature of 230 K.

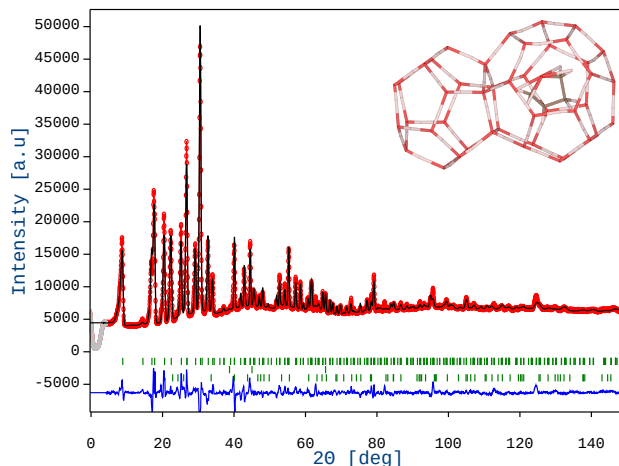


Figure 1: Diffraction pattern of fully deuterated THF-hydrates ( $\text{TDF} \cdot \text{D}_2\text{O}$ ) formed in situ taken on  $\text{D}_2\text{O}$  with  $\lambda = 1.546 \text{ \AA}$  at a temperature of 230 K (red) and the corresponding multi-phase Rietveld-refinement (black). See text for experimental conditions. The experimental data is available in Ref. [28]. The blue line depicts the difference between the data and the fit. The calculated peak positions (green ticks) correspond to phases considered for the refinement, which are, besides the TDF-hydrate, the aluminum sample environment and residual hexagonal ice (see section 2.2.1) for details on the refinement). The upper right corner shows 1 of the 8 large cages ( $5^{12} 6^4$ ) within the unit cell hosting a TDF molecule, as well as 1 of the 16 empty small cages ( $5^{12}$ ).

### 2.2.1 Structural Details

Data analysis and structure refinement were performed in the program Fullprof [29] [30]. A multi-phase Rietveld-refinement (see e.g. [31]) yields the lattice constants, the positional and thermal parameters, as well as the weight

Phase	TDF · D <sub>2</sub> O	Ice I <sub>h</sub>
Crystal System	cubic	hexagonal
Space Group	F d -3 m	P 63/m m c
Cell parameters	a = 17.22(7)	a = b = 4.50(7) c = 7.35(4)
R <sub>B</sub>	10.49	27.92
R <sub>wp</sub>	4.89	4.89

Table 3: Refinement details of the diffraction pattern depicted in figure 1. The Bragg R-factor (R<sub>B</sub>) and the weighted profile R-factor (R<sub>wp</sub>) indicate an acceptable fit.

percentage for each crystalline phase present in the sample. In a full refinement procedure the instrumental and background parameters are determined concurrently to the structure, the respective scale factors and the phase fractions. The TDF molecule was treated as a rigid body, with its position and the orientation within the large cage as free parameters. Aside from the phase under investigation (TDF-hydrates), the refinement includes the aluminum of the sample environment and residual hexagonal ice. The weight percentage  $W_j$  for the phase  $j$  can be calculated as in [32]:

$$W_j = \frac{S_j Z_j M_j V_{cj}}{\sum_i^N S_i Z_i M_i V_{ci}}, \quad (1)$$

with  $S$ ,  $Z$ ,  $M$  and  $V$  being the scale factor, the number of formula units per unit cell, the mass of one formula unit and the unit-cell volume, for each phase  $j$  and  $i$ , respectively. Fullprof also accounts for the multiplicities of each site, for occupation numbers unequal to 1, via the factor  $f_j$ , and the micro absorption of neutrons (Brindley factor  $t_j$ ) of each phase (see Ref. [33] for details):

$$W_j = \frac{S_j Z_j f_j^2 M_j V_j / t_j}{\sum_i^N S_i Z_i f_i^2 M_i V_i / t_i} = \frac{S_j \cdot \text{ATZ} \cdot V_j}{\sum_i^N S_i \cdot \text{ATZ}_i \cdot V_i},$$

with  $\text{ATZ} = Z_j f_j^2 M_j / t_j$ . (2)

Since our hydrate is stoichiometric ( $f_j = 1$ ) and the two phases in question have very similar absorption ( $t_j \sim 1$ ), equation 2 reduces to equation 1.

Depending on the sample, a clathrate weight percentage of  $95.1 \pm 1.5 \%$  to  $98.4 \pm 1.6 \%$  was reached for the samples investigated, with the uncertainty being dominated by the quality of the fit. In that context, it is important to note that deviations derived in these kinds of least-squares methods only partly reflect systematic errors which might be introduced by the instrument or sample. The details of the refinement are given in table 3. The fit suffers substantially from the size of the crystallites due to texture resulting from the in situ formation. Nevertheless, it provides evidence that the clathrate structure is formed with reliable purity from the liquid stoichiometric mixture.

### 2.3 Time of flight spectroscopy

After having confirmed the CS-II structure of the samples solidified by quenching or slower cooldown within

the cryostat we proceeded to study their low-energy excitations. To this end, experiments on the ILL time of flight (TOF) spectrometers IN5 [34] and Panther [35] were conducted. The goal of these experiments was to measure the dynamic structure function  $S(q, \omega)$  over a large fraction of  $(q, \omega)$ -space, which is made possible by the wide and complementary kinematic range of those two instruments. The analyzed data of these measurements will finally allow bench-marking density functional theory (DFT) and molecular dynamics (MD) simulations (elaborated in Ref. [19]). The four samples described in table 2 were measured under the configurations summarized in table 4. Additional measurements of each empty sample holder were conducted in order to subtract their contribution from the respective scattering signal. Vanadium standards were used to normalize our data to absolute units. Particular emphasis was put on selecting the geometries of the sample and the standard as identical as possible. By choosing thin hollow cylinders (with a wall thickness of  $d = 0.05$  mm for the partly or fully protonated samples and  $d = 0.1$  mm for the fully deuterated one) as sample geometry the multiple scattering was reduced to a minimum [36]. Note that unlike at D20, the sample containers are made from aluminum. The respective vanadium standard was cut from a sheet of the same thickness and placed inside the sample container without overlap. The vertical intensity profile of the beam was mapped out prior to the measurements. This allowed us to place the samples and the vanadium standards in the intensity distribution such as to minimize potential systematic effects due to possible small differences in their vertical extensions.

Instrument	Panther	IN5
Incident wavelength $\lambda_i$ [Å]	1, 2	2, 3
Incident energies $E_i$ [meV]	76, 19	19, 9
Temperature [K]	1.5	1.5

Table 4: Configurations for measurements conducted on ILL's TOF spectrometers. The overlap between incident wavelength allows crosschecking of the absolute units calibration.

Data reduction, analysis and visualization was done with the software package Mantid [37] [38]. Self-attenuation effects in the sample and the vanadium standard were calculated using a Monte Carlo simulation as described in [39]. The scattering of the sample environment was taken care of by subtracting measurements of the empty sample container in the cryostat. In order to normalize  $S(q, \omega)$  to absolute units, the data is multiplied by a factor  $f$ , derived from the vanadium standard:

$$f = \frac{N_V \sigma_V}{N_S}. \quad (3)$$

Therein,  $N_V$  is the number density and  $\sigma_V$  the total scattering cross section of vanadium and  $N_S$  the number density of the sample.  $N_V$  and  $\sigma_V$  are well known tabulated values, while  $N_S$  can be calculated from the structure given above. Note that it is essential for this method to know exactly the

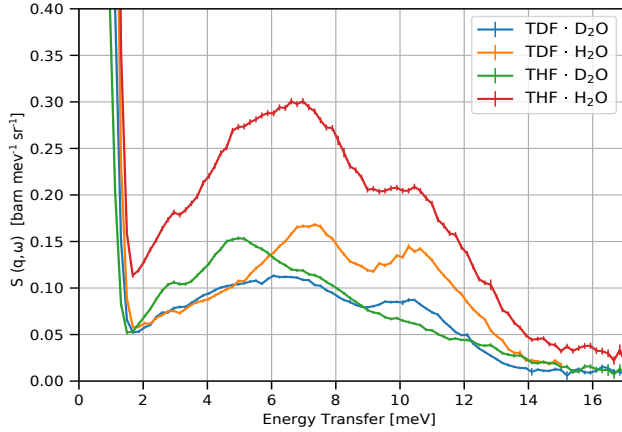


Figure 2: Constant  $q$ -slice at  $q = (4 \pm 1) \text{ \AA}^{-1}$  through  $S(q, \omega)$  for different deuteration and protonation of the THF-hydrate measured at **Panther** with an incident energy  $E_i = 19 \text{ meV}$  at a temperature of  $T = 1.5 \text{ K}$ . The characteristic peaks at 7 meV and 10.5 meV of CS-II can be well discerned. Preliminary results, data is available under [40].

purity and geometry of both the sample and the vanadium standard.

### 2.3.1 Low-energy excitations of THF-hydrates

Figure 3 and figure 2 show two spectra for different THF hydrate samples measured at IN5 and Panther. These spectra are obtained by integration over a given  $q$ -range, providing an average of the coherent signal in this range.

In the investigated energy region the dynamics of the host structure are dominated by the translational modes of the  $\text{H}_2\text{O}$  or  $\text{D}_2\text{O}$  molecule. This leads to two characteristic peaks at about 7 meV and 10.5 meV of every CS-II hydrate structure (see e.g. Ref. [41],[42],[14],[16],[43]), which can also be observed in figure 2 for both the protonated and the deuterated host structures. The most pronounced peaks are visible in the TDF ·  $\text{H}_2\text{O}$  sample (orange), as the contribution of the deuterated guest molecule is suppressed. The excitations of the guest molecule are located at lower energy and show very distinct peaks at about 2.9 meV and 4.7 meV, best visible in the THF ·  $\text{D}_2\text{O}$  sample (green) in figure 3. These localized excitations are particularly promising for moderation to the VCN range. As expected, they are shifted to slightly lower energies when substituting hydrogen with deuterium due to the increased mass and thus moment of inertia. This is the case for both translational modes of the host lattice and the excitations of the THF molecule, and consistent with phonon density of states (PDOS) computed by our collaborators [19].

## 3 Conclusions

VCN sources that deliver higher fluxes of very slow neutrons than current "standard" liquid deuterium sources could provide a powerful new tool for the neutron scattering community in the investigation of mesoscopic structures (e.g. in SANS), as well as tiny energy transfers

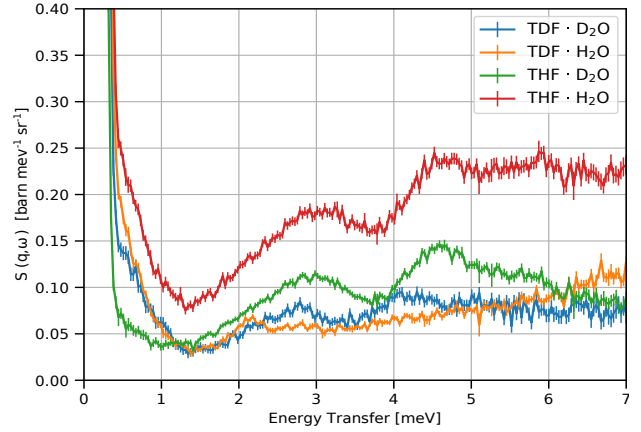


Figure 3: Constant  $q$ -slice at  $q = (3.5 \pm 0.75) \text{ \AA}^{-1}$  through  $S(q, \omega)$  for different deuteration and protonation of the THF-hydrate measured at **IN5** with an incident energy  $E_i = 9 \text{ meV}$  at a temperature of  $T = 1.5 \text{ K}$ . The observed peaks are due to localized excitations of the THF molecules (see text). The shoulder of the elastic peak is not a feature of the sample but back scattering of the sample environment. Preliminary result, data is available under Ref. [28].

(e.g. in NSE). This holds potential for bringing valuable advantages to the fields of soft condensed matter and structural biology. Furthermore they could play a significant role in increasing the sensitivity of particle physics experiments that employ beams of slow neutrons.

This work presented preliminary experimental results necessary for the development of VCN moderators using fully deuterated clathrate hydrates as a moderation material. In particular, a characterization of the structure and low-energy dynamics of THF-hydrates is elaborated. We have demonstrated that producing these hydrates is straightforward, and we were able to investigate localized, low-energy excitations using a method that involves contrast variation through partial or complete deuteration of the sample's constituents. The experimental determination of their dynamic structure factor  $S(q, \omega)$  in absolute units provides an important benchmark for scattering kernels developed within the HighNESS project. Together, these works shall enable reliable simulations of future neutron moderators using fully deuterated clathrate hydrates as a moderating medium. Additionally, these experiments serve as a baseline for future experiments on binary clathrate hydrates with both THF and molecular oxygen as guest molecules ( $17\text{D}_2\text{O}:\text{C}_4\text{D}_8\text{O}:\sim 2\text{O}_2$ ).

## 4 Acknowledgement

We would like to thank the HighNESS collaboration, particularly Shuqi Xu from the European Spallation Source and Sara Isaline Laporte from the University of Milano-Bicocca for many inspiring discussions. This work was funded by the HighNESS project within the European Framework for Research and Innovation Horizon 2020, under grant agreement 951782.

## References

- [1] F. Mezei, *Journal of Neutron Research* **24**, 205 (2023)
- [2] D.G. Phillips II, W.M. Snow et al., *Physics Reports* **612**, 1 (2016)
- [3] F.M. Piegsa, *Phys. Rev. C* **88**, 045502 (2013)
- [4] F.M. Piegsa, G. Pignol, *Physical Review Letters* **108**, 181801 (2012)
- [5] R. Golub, J. Pendlebury, *Physics Letters A* **53**, 133 (1975)
- [6] S. Degenkolb, P. Fierlinger, O. Zimmer, *Journal of Neutron Research* **24**, 123 (2023)
- [7] I.I. Gurevich, *Low-energy neutron physics* (North-Holland, Amsterdam, 1968)
- [8] D. Evans, *Cryogenics* **35**, 763 (1995), Nonmetallic Materials and Composites at Low Temperature-VII
- [9] E. Kulagin, S. Kulikov, V. Melikhov, E. Shabalin, *Nuclear Instruments and Methods in Physics Research B* **215**, 181 (2004)
- [10] M.H. Parajon, E. Abad, F. Bermejo, *Physics Procedia* **60**, 74 (2014)
- [11] G. Škoro, G. Romanelli, S. Rudić, S. Lilley, F. Fernandez-Alonso, *EPJ Web of Conferences* **239**, 17008 (2020)
- [12] I. Natkaniec, K. Holderna-Natkaniec, J. Kalus, *Physica B: Condensed Matter* **350**, E651 (2004)
- [13] A.K. Sum, C.A. Koh, E.D. Sloan, *Industrial & Engineering Chemistry Research* **48**, 7457 (2009)
- [14] H. Conrad, W.F. Kuhs, K. Nünighoff, C. Pohl, M. Prager, W. Schweika, *Physica B: Condensed Matter* **350**, E647 (2004)
- [15] V. Ananiev, et al., *Nuclear Instruments and Methods in Physics Research Section B: Beam Interactions with Materials and Atoms* **320**, 70 (2014)
- [16] M. Celli, D. Colognesi, L. Ulivi, M. Zoppi, A.J. Ramirez-Cuesta, *Journal of Physics: Conference Series* **340**, 012051 (2012)
- [17] O. Zimmer, *Physical Review C* **93**, 035503 (2016)
- [18] V. Santoro et al., *Development of a high intensity neutron source at the european spallation source: The highness project* (2022), <https://doi.org/10.48550/arXiv.2204.04051>
- [19] S. Xu, S.I. Laporte et al., *Theoretical calculations of neutron scattering cross sections for tetrahydrofuran-containing clathrate hydrates at low temperature* (Garching, Germany, 2023)
- [20] R. Macfarlane, D.W. Muir, R.M. Boicourt, A.C. Kahler, III, J.L. Conlin (2017)
- [21] X.X. Cai, T. Kittelmann, *Computer Physics Communications* **246**, 106851 (2020)
- [22] P. Willendrup, E. Farhi, K. Lefmann, *Physica B: Condensed Matter* **350**, E735 (2004)
- [23] P.K. Romano, N.E. Horelik, B.R. Herman, A.G. Nelson, B. Forget, K. Smith, *Annals of Nuclear Energy* **82**, 90 (2015), Joint International Conference on Supercomputing in Nuclear Applications and Monte Carlo 2013
- [24] J.T. Goorley, M.R. James et al., Tech. Rep. LA-UR-13-22934, 1086758 (2013)
- [25] T. Sato, Y. Iwamoto, S. Hashimoto, T. Ogawa, T. Furuta, S. Ichiro Abe, T. Kai, P.E. Tsai, N. Matsuda, H. Iwase et al., *Journal of Nuclear Science and Technology* **55**, 684 (2018)
- [26] S.R. Gough, D.W. Davidson, *Canadian Journal of Chemistry* **49**, 2691 (1971)
- [27] E.D. Sloan, C.A. Koh, *Clathrate Hydrates of Natural Gases.*, 3rd edn. (CRC Press, Taylor & Francis, Berkeley, California, 2008), ISBN 978-0-8493-9078
- [28] O. Zimmer et al., <https://doi.ill.fr/10.5291/ILL-DATA.1-10-42> (2020)
- [29] J. Rodríguez-Carvajal, *Physica B: Condensed Matter* **192**, 55 (1993)
- [30] J. Rodríguez-Carvajal, *IUCr Newsl.* **26** (2001)
- [31] R. Young, *The Rietveld method*, International Union of Crystallography. Monographs on Crystallography 5 (Oxford Univ. Press, Oxford [u.a.], 1993), ISBN 0198555776
- [32] R.J. Hill, C.J. Howard, *Journal of Applied Crystallography* **20**, 467 (1987)
- [33] J. Rodríguez-Carvajal, *An introduction into the program fullprof 2000 (version july 2001)* (2001)
- [34] J. Ollivier, M. Zbiri, J. Halbwachs, *Instrument layout: Disk chopper time-of-flight spectrometer IN5*, <https://www.ill.eu/users/instruments/instruments-list/in5>
- [35] B. Fak, M.M. Koza, O. Meulien, *Instrument layout: Thermal neutron time-of-flight spectrometer PANTHER*, <https://www.ill.eu/users/instruments/instruments-list/panther>
- [36] J. Wuttke, *Physica B: Condensed Matter* **266**, 112 (1999)
- [37] Mantid, *Manipulation and analysis toolkit for instrument data. mantid project*, <http://dx.doi.org/10.5286/SOFTWARE/MANTID> (2013)
- [38] O. Arnold, J. Bilheux, J. Borreguero, A. Buts, S. Campbell, L. Chapon, M. Doucet, N. Draper, R.F. Leal, M. Gigg et al., *Nuclear Instruments and Methods in Physics Research A* **764**, 156 (2014)
- [39] Mantid, *Mantid documentation. algorithm contents*, <https://docs.mantidproject.org/nightly/algorithms/index.html> (2023)
- [40] O. Zimmer et al., <https://doi.ill.fr/10.5291/ILL-DATA.1-10-49> (2021)
- [41] B. Chazallon, H. Itoh, M. Koza, W.F. Kuhs, H. Schober, *Phys. Chem. Chem. Phys.* **4**, 4809 (2002)
- [42] H. Schober, H. Itoh, A. Klapproth, V. Chihaiia, W. Kuhs, *The European Physical Journal E, Soft matter (Print)* **12**, 41 (2003)
- [43] D. Broseta, L. Ruffine, A. Desmedt, eds., *Gas Hydrates 1: Fundamentals, Characterization and Modeling*, 1st edn. (John Wiley & Sons, Inc., Hoboken, NJ, USA, 2017), ISBN 978-1-119-33268-8

